Geotextiles and Geomembranes 33 (2012) 25–33

Contents lists available at SciVerse ScienceDirect

Geotextiles and Geomembranes

journal homepage: www.elsevier.com/locate/geotexmem

Temperature effects on the swelling capacity and barrier performance of geosynthetic clay liners permeated with sodium chloride solutions

Hiroyuki Ishimori [a,1], Takeshi Katsumi [b,*]

[a] Research Center for Material Cycles and Waste Management, National Institute for Environmental Studies, Tsukuba, Ibaraki, 305-8506, Japan
[b] Graduate School of Global Environmental Studies, Kyoto University, Sakyo, Kyoto 606-8501, Japan

ARTICLE INFO

Article history:
Received 2 April 2011
Received in revised form
7 November 2011
Accepted 7 February 2012
Available online 24 April 2012

Keywords:
Bentonite
Hydraulic conductivity
Swelling
Temperature dependence

ABSTRACT

This paper examines the swelling capacity and hydraulic performance of geosynthetic clay liners (GCLs) at different temperatures against sodium chloride (NaCl) solutions. Free swell tests were conducted with deionized water and the NaCl solutions of 0.1–0.4 M. Permeating tests with the 0.4 M NaCl solutions were conducted using soil columns, which consisted of a GCL and underlying base layer soil similar to that in the bottom liner system in a landfill. The measured intrinsic permeabilities of the GCL to the 0.4 M NaCl solution are 5.9×10^{-18} m^2 for 20 °C and 2.5×10^{-17} m^2 for 60 °C, while the measured free swells to the solution are 8.5 mL/2 g for 20 °C and 11 mL/2 g for 60 °C and the free swells to other solutions tested also increase as the temperature increases. Even after accounting for the temperature dependence of the kinematic viscosity of the NaCl solutions, the intrinsic permeability increases with temperature because bentonite swelling depends on temperature. However, the free swell of bentonites in the GCLs increases as the temperature increases, and the relationship between free swelling and the permeability differs from the common notion that permeability decreases as the free swell increases. Consequently, the previous relationships obtained from free swell tests and hydraulic conductivity tests at room temperature are not applicable at elevated temperatures because at elevated temperatures, the increased intrinsic permeability is related to the decreased swelling pressure.

1. Introduction

Composite liners consisting of geomembranes (GMs) overlying geosynthetic clay liners (GCLs) or compacted clay liners (CCLs) are widely used in barrier systems (Chien et al., 2006; Müller, 2007). In the case of composite liners, even when GMs are damaged and their barrier performance is degraded, the underlying GCLs or CCLs can act as barrier materials against waste leachates. Because GCLs or CCLs represent the final defense against groundwater contamination due to leakage of landfill leachates, clarifying their physical properties and barrier performance in landfill environmental conditions is important. Many studies have focused on the properties of the bentonite component of GCLs and CCLs. Their studies have investigated the effects of (1) varying chemical constituents and concentrations in permeating solutions (Jo et al., 2001; Shan and Lai, 2002; Kolstad et al., 2004a; Katsumi et al., 2007), (2) the type and quality of the bentonite (Onikata et al., 1996; Gates et al., 2004; Kolstad et al., 2004b; Lee and Shackelford, 2005a; Katsumi et al., 2008b) (3) overburden pressure (Petrov and Rowe, 1997; Katsumi and Fukagawa, 2005), (4) prehydration or initial water content (Daniel et al., 1993; Vasko et al., 2001; Lee and Shackelford, 2005b; Katsumi et al., 2008a), and (5) temperature (Cho et al., 1998, 1999; Bouazza et al., 2008).

Organic substances within landfill waste biologically decompose, and the temperature inside a landfill can reach about 60 °C from biologically generated heat (Yoshida et al., 1996; Rowe, 2005; Yesiller et al., 2005; Koerner and Koerner, 2006). Temperature effects on swelling capacity and subsequent hydraulic performance of GCLs to waste leachates has yet to be sufficiently investigated. Most of the previous studies have focused on desiccation cracks, deformation, and hydraulic properties to deionized water on the bentonite (Southen and Rowe, 2005a, 2005b; Cho et al., 1998, 1999; Bouazza et al., 2008; Jacinto et al., 2009), whereas only limited studies have evaluated the barrier performance at elevated temperature conditions (Ishimori et al., 2010). Thus, the effect of the high temperature conditions in a landfill on the barrier performance against waste leachate is still largely unknown.

* Corresponding author. Tel.: +81 75 753 9205; fax: +81 75 753 5116.
E-mail addresses: ishimori.hiroyuki@nies.go.jp (H. Ishimori), katsumi.takeshi.6v@kyoto-u.ac.jp (T. Katsumi).
[1] Tel.: +81 29 850 2278; fax: +81 29 850 2016.

0266-1144/$ – see front matter © 2012 Elsevier Ltd. All rights reserved.
doi:10.1016/j.geotexmem.2012.02.005

'This paper quantitatively demonstrates the effects of elevated temperature on the free swell and the hydraulic conductivity of GCLs. The free swell tests were conducted in deionized water and sodium chloride (NaCl) solutions of 0.1–0.4 M at 20 °C and 60 °C according to the ASTM D5890 (2006). The permeating tests, which consisted of a GCL and underlying base layer soil similar to that in a bottom liner system, were conducted to evaluate the hydraulic conductivity and the intrinsic permeability of GCL to the 0.4 M NaCl solution at 20 °C and 60 °C. The tests can investigate the barrier performance of the GCL and the solute transport phenomena in the underlying base layer soil under simulated landfill environmental conditions of suction of underlying unsaturated base layer soil, overburdened confining pressure, and vertical temperature distribution. Then, the results of the free swell and hydraulic conductivity tests are used to evaluate the effects of elevated temperature on the barrier performance against NaCl solutions.

2. Temperature effects on swelling and permeability

Swelling and permeability of bentonite materials are likely to depend on temperature according to the following considerations. Swelling is associated with the thickness of the diffusion double layer (DDL) of a bentonite particle as follows (Yeung, 1992; Mitchell, 1993; Studds et al., 1996; Gleason et al., 1997).

$$\theta = \sqrt{\frac{\varepsilon_0 \kappa RT}{2F^2 c v^2}} \tag{1}$$

where θ is the Debye length (m), ε_0 is the vacuum permittivity (8.86×10^{-12} F/m), κ is the relative permittivity of the pore fluid, R is the universal gas constant (8.134 J/mol/K), T is the absolute temperature (K), F is Faraday's constant (9.65×10^4 C/mol), c is the pore-fluid concentration (mol/m^3), and v is the valence of the counter ion. Mitchell (1993) indicates that the effects of temperature on the DDL thickness are slight because the permittivity decreases as the temperature increases; $\kappa = 81.2$ for 20 °C and $\kappa = 67.6$ for 60 °C to water (Schwanka et al., 2006). But, how the slight change of the DDL thickness affects the free swell has not been quantitatively clarified.

Temperature effects on the permeability are well known. The hydraulic conductivity depends on temperature as follows (Bear, 1972).

$$k = K\frac{\rho g}{\mu} = K\frac{g}{\nu} \tag{2}$$

where k is the hydraulic conductivity (m/s), K is the intrinsic permeability (m^2), ρ is the fluid density (kg/m^3), μ is the fluid viscosity (Pa s), ν is the kinematic viscosity (m^2/s), and g is the gravitational acceleration (9.81 m/s^2). The hydraulic conductivity increases with temperature because the kinematic viscosity decreases as the temperature increases.

A few studies have examined the influence of temperature on the hydraulic conductivity of bentonites. For example, Cho et al. (1999) investigated the effects of temperature on the hydraulic conductivity of compacted calcium bentonites to deionized water. Bouazza et al. (2008) studied the influence of temperature between 20 and 60 °C on the volumetric change and hydraulic conductivity of GCLs with sodium bentonites to deionized water. Although the hydraulic conductivity in both of these studies increased with temperature, the increase was dominated by the temperature dependence of the kinematic viscosity.

When deionized water is used as a permeating solution, the swelling due to deionized water is so significant that the temperature effects on the hydraulic conductivity are likely dominated by the temperature dependence of the kinematic viscosity instead of the temperature dependence of swelling. For example, Katsumi et al. (2008b) have demonstrated the relationship between the hydraulic conductivity and the free swell at a confining pressure of 30 kPa. According to their study, the hydraulic conductivity of bentonites with a free swell greater than 15 mL/2 g was approximately $k = 1.0 \times 10^{-11}$ m/s (Fig. 1). The free swell of sodium bentonites in deionized water is about 30 mL/2 g (Egloffstein, 1995, 2001). Thus, the hydraulic conductivity may not reflect the temperature dependence of swelling when deionized water is used as the permeating solution. Because deionized water sufficiently swells bentonites, the hydraulic conductivity should be more influenced by the temperature dependence of the kinematic viscosity than the temperature dependence of the swelling. In contrast, bentonites permeated with electrolytic chemical solutions such as waste leachates typically do not swell as much as those in deionized water (Norrish, 1954; Norrish and Quirk, 1954; Posner and Quirk, 1964; Slade and Quirk, 1990; Slade et al., 1991). Consequently, in these insufficiently swollen bentonites the influence of temperature on swelling and hydraulic conductivity will be more evident.

As described above, previous studies employed deionized water as the permeating solution to investigate the temperature effects on the hydraulic conductivity of bentonites. However, their studies were probably conducted under conditions where the temperature dependence of the kinematic viscosity affects the hydraulic conductivity more strongly than the temperature dependence of the swelling. Thus, to clarify how the temperature dependence of swelling affects the hydraulic conductivity, employing an electrolytic chemical solution as a permeating solution would be more effective, because insufficiently swollen bentonites are more sensitive to temperature induced changes in the swelling volume than sufficient swelling bentonites (Fig. 1). Moreover, using an electrolytic chemical solution similar to waste leachates is important to evaluate the barrier performance under conditions similar to those in landfill environments.

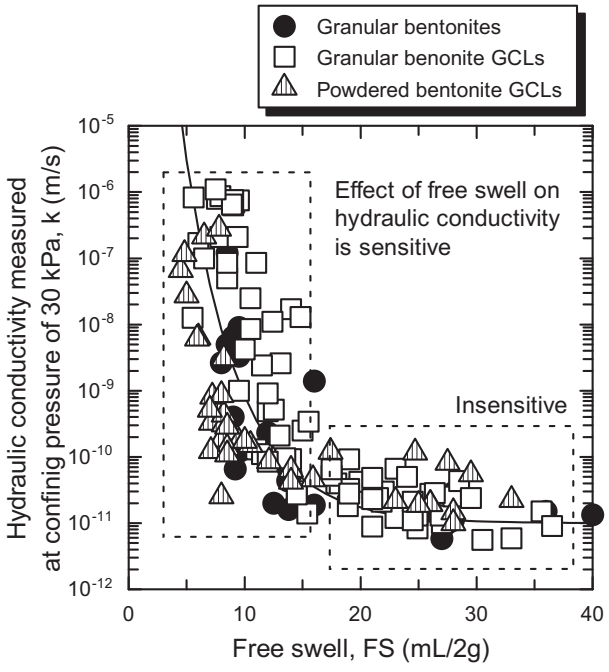

Fig. 1. Effect of free swell on hydraulic conductivity (modified Katsumi et al., 2008b).

3. Materials and methods

3.1. Free swell tests

The bentonites used in the tests were removed from a typical GCL (Bentofix NSP 4900-1, NAUE GmbH & Co. KG) where powdered sodium bentonite was encapsulated between a polypropylene woven geotextile and a polypropylene nonwoven geotextile by needle-punching fibers. The soil particle density was 2.65 g/cm^3 (JIS A1202, 2009), the liquid limit was 466% (JIS A1205, 2009), and the methylene blue consumption was 82 mmol/100 g (JBAS-107, 1991). Table 1 summarizes the physical properties of the bentonites. The permeating solutions used in free swell tests were: (1) deionized water, (2) 0.1 M NaCl solution, (3) 0.2 M NaCl solution, and (4) 0.4 M NaCl solution. The NaCl concentrations used as the permeating solutions have realistic electric conductivity compared to the concentrations of waste leachates. The electric conductivity of the 0.4 M NaCl solution is about 3,270 mS/m, and the electric conductivity of the waste leachates reported in Yasuhara et al. (1997) and Kjeldsen et al. (2002) is 3,890 mS/m at maximum. The testing temperatures were 20 °C and 60 °C.

The free swell tests were conducted according to ASTM D5890 (2006). First, 2 g of dry powdered bentonite was dusted into in a 100 mL graduated cylinder filled with 90 mL of solution, which was heated to 20 °C or 60 °C. Then after dusting of bentonite was complete, the cylinder was filled to 100 mL with the permeating solution. The graduated cylinder then was carefully placed in a room controlled at 20 °C or in the constant temperature bath controlled at 60 °C, and the cylinder remained undistributed for 24 h prior to the first reading. In the 60 °C testing case, paraffinic mineral base oil with an extremely limited solubility was floated on the surface of the permeating solution in the cylinder to prevent evaporation.

3.2. Permeating tests

Fig. 2 schematically depicts the permeating tests where the column consisted of an acrylic mold and stainless steel upper and lower cylinders. The 0.6 m high acrylic mold had a 0.06 m inner diameter. The base layer soil was simulated by packing the mold with decomposed granite soil. A GCL specimen was set in the bottom cylinder, which had the same inner diameter as the mold, and the GCL with the bottom of the mold was fixed to the top of the acrylic mold. The upper cylinder was placed in the bottom cylinder, and could vertically move up and down in the bottom cylinder like a piston. The load of 30 kPa on the top of the upper cylinder acted as the confining pressure on the GCL specimen while the thickness and change in the GCL were measured from the displacement of the upper cylinder. Permeating solution was injected from a burette pipe, which was connected to the upper cylinder, and the solutions were warmed to 20 °C or 60 °C by a heat rod attached on the cylinder.

Table 1
Properties of bentonite used.

Property	Unit	Standard	Value
Soil particle density	g/cm^3	JIS A1202	2.65
Natural water content	%	JIS A1203	7.6
Liquid limit	%	JIS A1205	466
Methylene blue consumption	mmol/100 g	JBAS 107	82.0
Free swell to deionized water	mL/2 g	ASTM D5890	30.0
Free swell to 0.4 M NaCl solution	mL/2 g	ASTM D5890	8.5
Hydraulic conductivity to deionized water	m/s	ASTM D5084	2.01×10^{-11}
Hydraulic conductivity to 0.4 M NaCl solution	m/s	ASTM D5084	1.09×10^{-10}

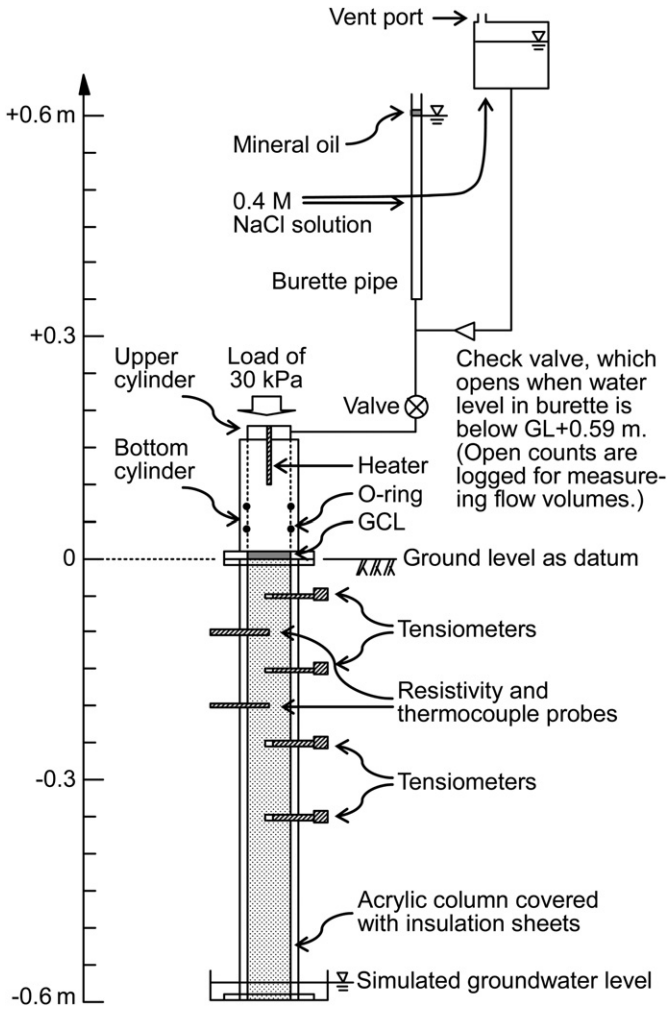

Fig. 2. Schematic of permeating test.

Detailed setup procedures are described as follows. First, decomposed granite soil with a 10% water content was packed into the acrylic column, and then the soil was homogeneously compacted to achieve to a bulk dry density of 1.95 g/cm^3. Table 2 shows the properties of the decomposed granite soil. The acrylic column had ports to attach sensors at 0.05 m intervals. The top of the column was referred to as the ground level (GL) for datum, and tensiometers (Microtensiometer SK-5500-M6, Sankeirika Inc.) were installed at GL-0.05 m, GL-0.15 m, GL-0.25 m, GL-0.35 m in

Table 2
Properties of decomposed granite soil.

Property	Unit	Standard	Value
Soil particle density	g/cm^3	JIS A1202	2.68
Natural water content	%	JIS A1203	0.45
Optimum water content	%	JIS A1210	10.9
Hydraulic conductivity	m/s	JIS A1218	3.73×10^{-7}
Soil pH[a]	–	JGS 0211	7.93
Soil electric conductivity[a]	mS/m	JGS 0212	1.94
Soil particle size distribution		JIS A1204	
>2,000 um	%		15.6
2000–75 um	%		69.1
75–5 um	%		12.7
<5 um	%		2.6

[a] pH and electric conductivity of the suspended solution when the soil (S) and the deionized water (L) are mixed at the liquid–solid ratio of $L/S = 5$.

order to measure the pore water pressures and evaluate the hydraulic conductivity of the GCL, while the resistivity probes with thermocouples (Microresistivity probe with four poles SK-3100, Sankeirika Inc.) were installed at GL-0.10 m and GL-0.20 m in order to estimate the pore water concentrations and the soil temperatures. The resistivity probe measures the apparent soil electrical resistance, which depends on the volumetric water content and the soil pore water electric conductivity as follows:

$$EC_a \equiv \frac{1}{a \cdot R_a} = EC_w \cdot \theta_w^2 \quad (3)$$

where, EC_a is the apparent electric conductivity (mS/m), R_a is the apparent soil electrical resistance (kΩ) as the sensor output, EC_w is the pore water electric conductivity (mS/m), θ_w is the volumetric water content, and a is the calibration constant (=0.043 m in this case). Finally, the acrylic column was covered with insulation sheets for the cut-off of the room temperature effects.

Next, the bottom cylinder was used as a consolidation mold to prepare the GCL specimen. The cylinder was first placed in a container, and a woven geotextile with the 0.06 m diameter was placed in the cylinder. Granular bentonite (23.4 g in dry weight) was loosely packed on the geotextile, and the upper woven geotextile was placed on top of the packed bentonite to sandwich the bentonite between two woven geotextiles like a GCL. The reason for not using a manufactured GCL was that trimming the manufactured GCL was so difficult that the interaction between the cylinder and the side of the heterogeneously trimmed GCL may have an influence on the friction and the permeability. The unit weight of the prepared GCL was 8,280 g/m^2, which is larger than that of typical GCL (Egloffstein, 1995, 2001). The container and the cylinder were then filled with a 0.4 M NaCl solution at room temperature. The GCL in the cylinder was hydrated with a 15 kPa confining pressure for a week. The 15 kPa confining pressure was required to fill a free space between the cylinder and the side of the GCL specimen and to avoid a leakage of the permeating solution during the tests. After hydration, the NaCl solution around the GCL specimen was removed, and the cylinder with the GCL specimen was fixed to the top of the acrylic column. The GCL in the cylinder had a void ratio of about 2.68 and a thickness of about 11.5 mm.

Lastly, the upper cylinder, which contained a stainless heat rod with a 0.02 m diameter and a 0.15 m length, was inserted into the bottom cylinder using O-rings. The heat rod was wired to a heater (Thermo-controller SBX-303, Sakaguchi E. H. Voc Corp.), which can keep the heat rod at a given constant temperature. The temperature of the permeating solution can be almost the same as that of the heat rod, because the flow velocity passing through the GCL was so slow that the permeating solution can retain in the cylinder enough for warming to the given temperature. The upper cylinder was connected with a burette through a tube possessing a valve, and then the burette was filled with the 0.4 M NaCl solution before initiating the permeating tests. The paraffinic mineral base oil with an extremely limited solubility was floated on the surface of the water level to prevent evaporation.

When the pore water pressure heads obtained from the tensiometers installed in the base layer were stable with time, the tests were initiated. The valve to the burette was opened, and the switch of the heater was turned on to warm the permeating solution to 20 °C or 60 °C. At the same time, a load was placed on the upper cylinder to confine the GCL with the effective pressure of 30 kPa. After the valve was opened, a 0.4 M NaCl solution was automatically added from an outside tank into the burette as needed to keep the water level in the pipe GL + 0.59 − 0.60 m, and the following items were monitored with time: (1) flow volumes which are equivalent to the volumes supplied through the open-close check value from the outside tank, (2) pore water pressure heads obtained from the tensiometers, (3) temperatures obtained from the thermocouples, and (4) apparent electric conductivities obtained from the resistivity probes. The tests were repeated twice for each temperature condition (20 °C or 60 °C). The purpose of the duplicates was to check the repeatability of the flow rates passing through the GCL.

4. Results

4.1. Free swells

Table 3 and Fig. 3 show the free swells in the solutions. The free swell is higher for permeating solutions with a lower concentration and a higher temperature. Free swell is related to DDL thickness. Table 3 includes the Debye length estimated from Eq. (1), assuming the relative permittivity is $\kappa = 81.2$ for 20 °C and $\kappa = 67.6$ for 60 °C to water (Schwanka et al., 2006). Fig. 4 shows the relationship between Debye length and free swell in the NaCl solutions. The free swell increases with the DDL thickness at the same temperature. The DDL thickness given from Eq. (1) is useful to estimate the effects of the electrolyte on the free swell at the same temperature. In contrast, when the temperature increases from 20 °C to 60 °C, the free swell increases as the thickness becomes thin. Therefore, it may be difficult to estimate the temperature effect on the free swell using the DDL thickness given in Eq. (1).

4.2. Flow and transport in GCL and underlying soil

Table 4 summarizes the results of the permeating tests, including the properties such as thickness, bulk density, void ratio, and hydraulic conductivity of the GCLs before and after permeation. In the table, "GCL_X (Y)" means the Yth permeating test for 0.4 M NaCl permeation with temperature of X °C. Fig. 5 shows the changes in cumulative flow volumes passing through the GCLs with time. For all tests, the cumulative flow volumes linearly increase with time. The flow velocity can be estimated by dividing the slope in this figure into the area of GCLs. The calculated flow velocities are 6.4×10^{-9} m/s for $GCL_{20}(1)$, 5.2×10^{-9} m/s for $GCL_{20}(2)$, 3.1×10^{-8} m/s for $GCL_{60}(1)$, and 3.4×10^{-8} m/s for $GCL_{60}(2)$. The flow velocities for each temperature condition clearly differ; the flow velocity for the 60 °C NaCl permeation is about six times larger than that for the 20 °C NaCl permeation.

Fig. 6(a) and (b) show the outputs of the tensiometers, resistivity probes, and thermocouples for the 20 °C and 60 °C NaCl permeations, respectively. In the case of NaCl permeation at 20 °C (hereafter 20 °C NaCl permeation), the readings from the pressure heads abruptly increase immediately after the permeation is initiated, but then gradually decrease with time. That means the soil column is getting gradually desiccated because of too limited flow volume passing through the GCL. In actuality, the top of the soil column when the test finished had the smaller water content than the initial water content, as shown in Fig. 7(a) later. During the permeation, the pressure heads remain within −0.37 m to −0.19 m;

Table 3
Results of free swell tests.

Permeating solution	20 °C		60 °C	
	Debye length (nm)	Free swell (mL/2 g)	Debye length (nm)	Free swell (mL/2 g)
Deionized water	–	30.0	–	35.0
0.1 M NaCl	0.959	15.0	0.875	19.0
0.2 M NaCl	0.678	11.5	0.619	14.0
0.4 M NaCl	0.480	8.5	0.438	11.0

Debye length was calculated from DDL theory of Eq. (1).

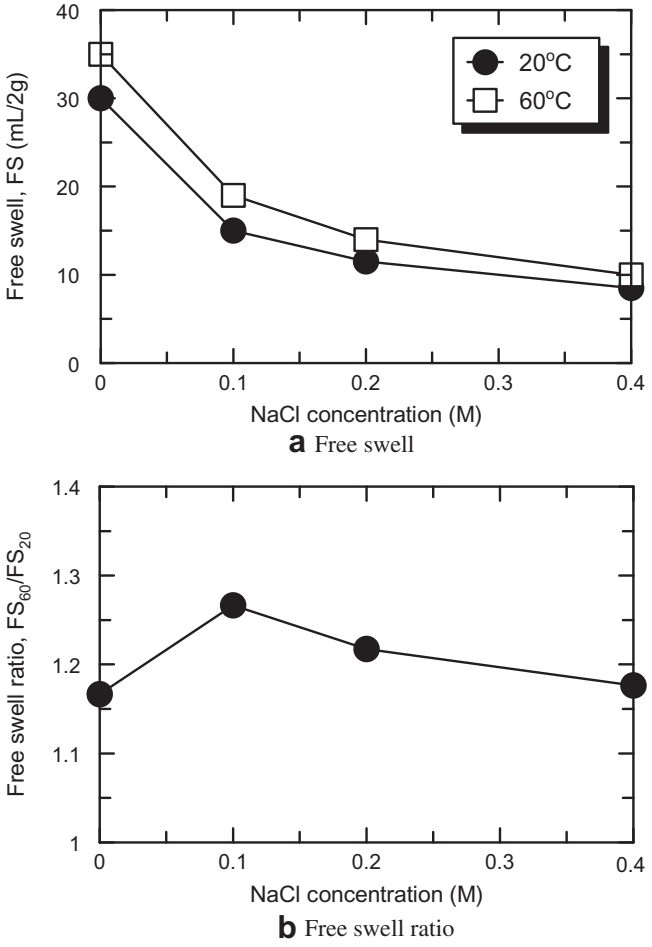

Fig. 3. Effect of temperature on free swell.

the pore water pressure in the soil column is −0.37 m at GL-0.05 m, −0.34 m at GL-0.15 m, −0.27 m at GL-0.25 m, and −0.19 m at GL-0.35 m on the 40th day. The responses of the resistivity probes depend on both the water content and NaCl concentration as shown in Eq. (3). Assuming the water content is constant at each sensor, the different resistivity probe responses indicate the change in the NaCl concentration. The apparent electric conductivity at GL-0.10 m reaches about 125 mS/m at the 20th day, which is equivalent

Table 4
Summary of permeation column tests.

	GCL_{20} (1)	GCL_{20} (2)	GCL_{60} (1)	GCL_{60} (2)
Testing condition				
Permeating solution	20 °C NaCl with 0.4 M		60 °C NaCl with 0.4 M	
Duration (day)	205	98	74	98
Sensors installation	No	Yes	No	Yes
Initial condition				
Thickness (mm)	11.54 (15.00)[a]			
Void ratio	2.68 (3.80)[a]			
Bulk dry density (g/cm^3)	0.72 (0.55)[a]			
Final condition				
Thickness (mm)	10.74	11.14	10.30	10.43
Void ratio	2.44	2.57	2.30	2.34
Bulk dry density (g/cm^3)	0.77	0.74	0.80	0.79
Water content (%)	104	121	111	86.9
Soil electric conductivity (mS/m)	–	3,130	–	9,330
Flow velocity (m/s)	6.4×10^{-9}	5.2×10^{-9}	3.1×10^{-8}	3.4×10^{-8}
Hydraulic conductivity (m/s)	–	5.8×10^{-11}	–	5.1×10^{-10}
Intrinsic permeability (m^2)[b]	–	5.9×10^{-18}	–	2.5×10^{-17}

[a] Values in brackets are for the GCL before preconsolidation of 15 kPa, and the values outside the brackets are for the GCL after preconsolidation.
[b] Estimated from the hydraulic conductivity and the water kinematic viscosity, including a temperature correction.

to the electric conductivity of the permeating solution (3,270 mS/m) because the pore water electric conductivity, EC_w, is calculated as $EC_a/(\theta_w^2)$ = 125 (mS/m)/0.20/0.20 = 3,130 mS/m where the volumetric water content is assumed 0.20 from the initial water content of 10%. Thus, it takes 20 days for the advective front of the permeating solution to reach GL-0.10 m. The temperatures in the base layer remain nearly constant at 20 °C, regardless of depth.

In the case of NaCl permeation at 60 °C (hereafter 60 °C NaCl permeation), the change of the pressure head is nearly the same regardless of depth. The readings of the pressure heads gradually increase with time; the pore water pressures are about −0.09 m on the 40th day. The 60 °C NaCl solution increases the flow volume from the GCL so that the underlying base layer is getting gradually saturated. The profiles of their pressure heads are the opposite of the 20 °C NaCl permeation case. The resistivity probe at GL-0.10 m responds sharper than that for the 20 °C NaCl permeation. The apparent electric conductivity reaches about 170 mS/m at the 40th day. As the electric conductivity generally increases with the temperature at the rate of 2%/°C, the apparent electric conductivity is corrected to 155 mS/m at 20 °C. Thus, the pore water electric conductivity is calculated as $EC_a/(\theta_w^2)$ = 155 (mS/m)/0.20/0.20 = 3,880 mS/m, and it is slightly higher

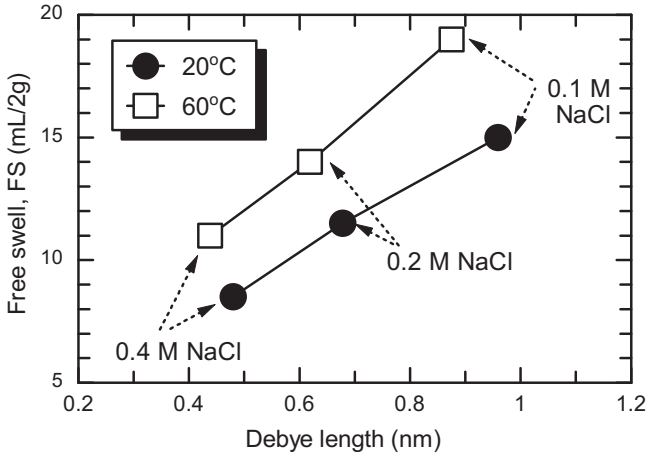

Fig. 4. Relationships between Debye length and free swell.

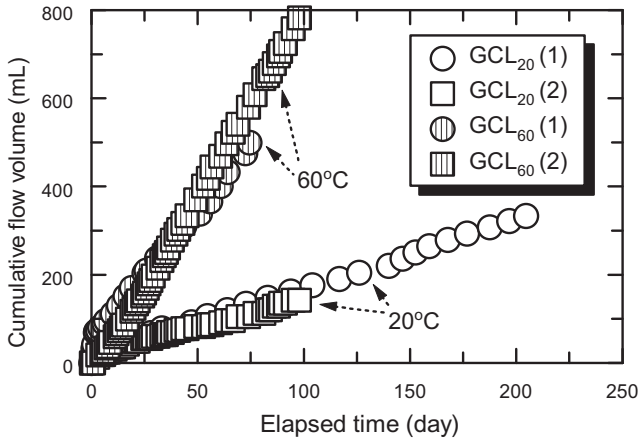

Fig. 5. Cumulative flow volumes passing through GCL specimens.

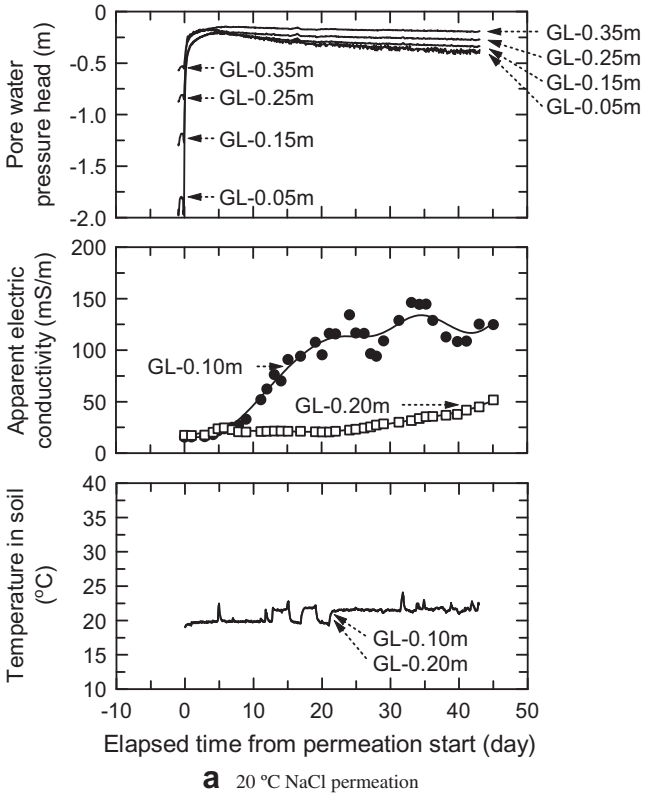

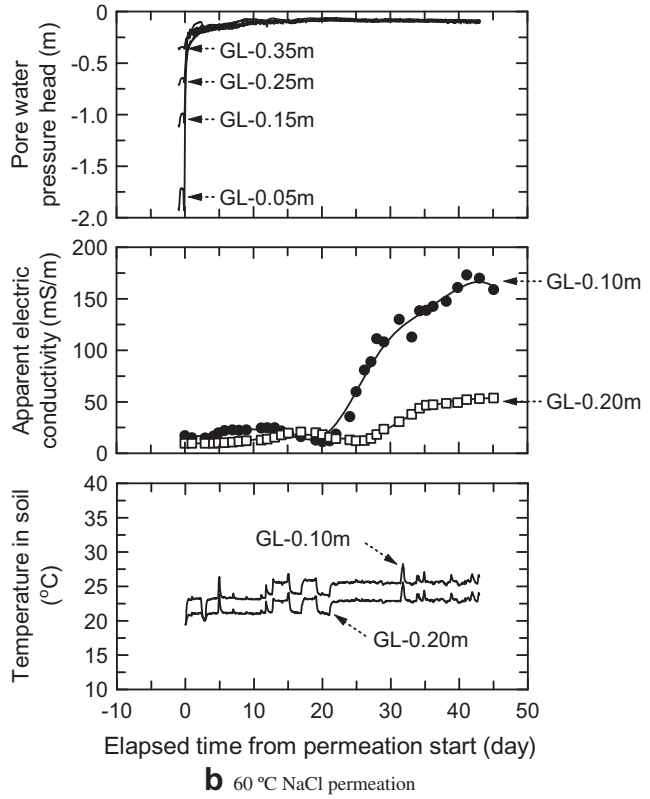

Fig. 6. Changes in pore pressure head, apparent electric conductivity, and temperature in base layer soil over time.

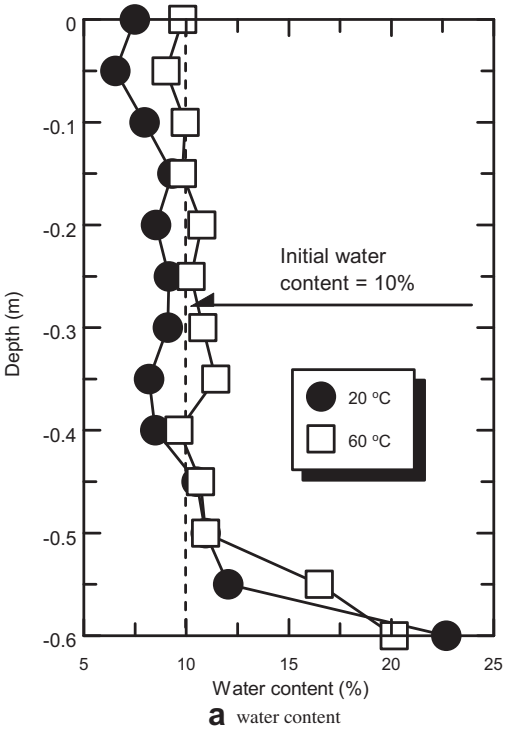

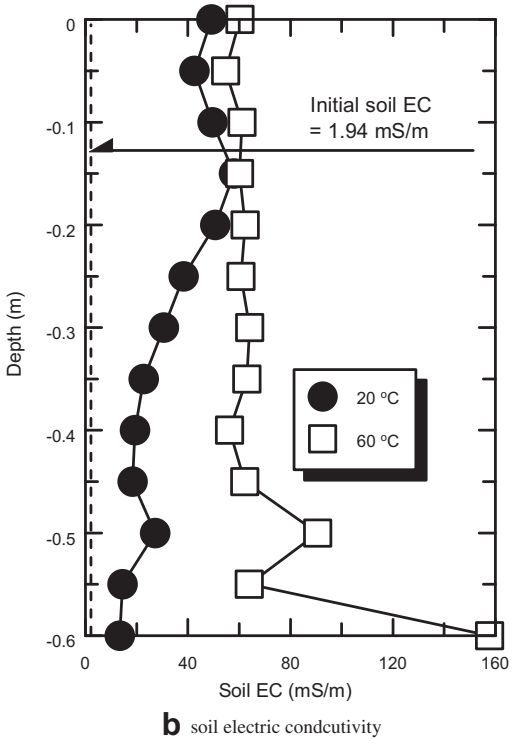

Fig. 7. Distribution of water content and soil electric conductivity in GCL and base layer soil.

than that of the permeating solution. The assumed volumetric water content of 0.20 may be underestimated because the flow volume passing through the GCL is higher in the 60 °C NaCl permeation than in the 20 °C NaCl permeation. Or, the NaCl concentration in the pore water may be increased due to the evaporation. It takes 40 days for the advective front of the permeating solution to reach GL-0.10 m. Regardless of the larger flow volume, the advective front reaches GL-0.10 later. One of the reasons is that the retardation effect due to the adsorption in the GCL is enhanced by the elevated temperature. Lastly, the temperatures in soil slightly increase due to the 60 °C NaCl permeation as there is a temperature gradient from GL-0.10 m to GL-0.20 m.

Fig. 7(a) and (b) show the distribution of the water content and the soil electric conductivity in the base layer soil upon completion of the permeating tests. The water content and the soil electric conductivity of the GCLs are included in Table 4. The soil electric conductivity is the electric conductivity of the suspended solution when the soil (S) and the deionized water (L) are mixed at the liquid–solid ratio of $L/S = 5$ according to JGS 0212 (2009). The soil in the base layer was sampled at 0.05 m intervals in the depth-direction. After desiccating the sampled soil to measure the water content, the desiccated soil was mixed with the deionized water five times the weight of the soil, and then the electric conductivity of the suspended solution was measured. In case of the GCL, the whole GCL was desiccated to measure the water content and the desiccated GCL was mixed with the deionized water five times the weight of the GCL in order to measure the electric conductivity of the GCL. The base layer soil has an initial water content of 10%. For the 20 °C NaCl permeation, the soil around the GCL has smaller water content than initial water content, and this is consistent with the tensiometer profiles as shown in Fig. 6(a). In contrast, the change in the water content is negligible after the tests for the 60 °C NaCl permeation. The water content at GL-0.60 m is high compared with the water contents at other depths because the bottom of base layer soil simulated the groundwater table. Although the base layer soil has an initial soil electric conductivity of 1.94 mS/m, the overall soil electric conductivity distribution in the base layer soil increases after the test for the 60 °C NaCl permeation. The soil electric conductivity profiles in the base layer soil reach a breakthrough, because the soil electric conductivity of 60 mS/m is approximately equivalent to the electric conductivity of the permeating solution. The pore water electric conductivity, EC_w, is calculated from the soil electric conductivity in JGS 0212 (2009) as follows; $EC_w = EC_a \times L/S \times \rho_d/\theta_w = 60\ (\mathrm{mS/m}) \times 5\ (\mathrm{mL/g}) \times 1.95\ (\mathrm{g/cm^3})/0.19 = 3{,}080\ \mathrm{mS/m}$, where ρ_d is the bulk dry density ($\mathrm{g/cm^3}$), L/S is the liquid–solid ratio in the measurement by JGS 0212 (2009), and the volumetric water content, θ_w, is 0.19 as the averaged value from GL-0.00 m to from GL-0.45 m as shown in Fig. 7. In contrast, the soil electric conductivity for the 20 °C NaCl permeation is high only around the GCL. The soil electric conductivity around the bottom of the base layer soil is as low as the initial value, indicating the concentration profiles in the base layer soil has yet to reach the breakthrough. As shown in Table 4, the GCL permeated with a higher temperature solution has a smaller water content, but a larger soil electric conductivity. The final thickness of the GCL is thinner for the 60 °C NaCl permeation than for the 20 °C NaCl permeation. Therefore, the GCL permeated with a higher temperature solution may have a smaller swelling pressure and inferior barrier performance.

4.3. Hydraulic conductivity

The hydraulic conductivity can be estimated from

$$\frac{d}{k_e} = \frac{d_{GCL}}{k_{GCL}} + \frac{d_{BASE}}{k_{BASE}} \tag{4}$$

where k_e is the equivalent hydraulic conductivity of the base layer soil and the GCL (m/s), d_{GCL} is the thickness of the GCL (m), d_{BASE} is the distance from the GCL to the installation point of the tensiometer at GL-0.05 m (m), d is the sum of the d_{GCL} and d_{BASE} (m), and k_{GCL} and k_{BASE} are the hydraulic conductivity values of the GCL and the base layer (m/s), respectively. The hydraulic conductivity of the GCL, k_{GCL}, can be estimated by evaluating the equivalent hydraulic conductivity, k_e, from the flow velocity and the pore water pressure head obtained by the tensiometer at GL-0.05 m. Namely, the equivalent hydraulic conductivity, k_e, is calculated as

$$k_e = \frac{q}{i} = \frac{qd}{d + h - h_w} \tag{5}$$

Therefore, the hydraulic conductivity of the GCL can be estimated from

$$k_{GCL} = d_{GCL}\left(\frac{d}{k_e} - \frac{d_{BASE}}{k_{BASE}}\right) = d_{GCL}\left(\frac{d + h - h_w}{q} - \frac{d_{BASE}}{k_{BASE}}\right) \tag{6}$$

where q is the flow velocity passing through the GCL specimen (m/s), i is the hydraulic gradient, h is the height of water level in the burette (0.6 m), and h_w is the pore water pressure head measured from tensiometer (m). The calculated hydraulic conductivity of the GCL is $k_{GCL} = 5.8 \times 10^{-11}$ m/s for the 20 °C NaCl permeation, and $k_{GCL} = 5.1 \times 10^{-10}$ m/s for the 60 °C NaCl permeation. Here the assumed hydraulic conductivity of the base layer soil is $k_{BASE} = 3.7 \times 10^{-7}$ m/s, which is the value for saturated soil. Although the underlying base layer soil is not fully saturated during the permeating tests, the assumption for the k_{BASE} value can reasonably estimate the k_{GCL} value because the k_{GCL} value is much smaller than the k_{BASE} value. In actuality, the difference of the assumed k_{BASE} value has a negligible effect on the estimated k_{GCL} value.

In addition, the intrinsic permeability can be calculated from the estimated hydraulic conductivity using Eq. (2) to remove the temperature dependence of the kinematic viscosity. The kinematic viscosities for the calculation are $\nu_{20} = 1.0 \times 10^{-6}$ $\mathrm{m^2/s}$ at 20 °C and $\nu_{60} = 4.8 \times 10^{-7}$ $\mathrm{m^2/s}$ at 60 °C. The calculated intrinsic permeability values of the GCLs are 5.9×10^{-18} $\mathrm{m^2}$ for the 20 °C NaCl permeation and 2.5×10^{-17} $\mathrm{m^2}$ for the 60 °C NaCl permeation. Table 4 summarizes the results.

4.4. Considerations

Even after considering the dependence of the kinematic viscosity, the permeating tests clarified that the intrinsic permeability to the NaCl solution is about four times higher at 60 °C than at 20 °C. This difference appears as a temperature effect on the intrinsic permeability using electrolytic chemical solutions, and this behavior differs from that of deionized water used in previous studies.

According to the free swell tests, the intrinsic permeability to the NaCl solution should be higher at 20 °C than at 60 °C because bentonites hydrated with a NaCl solution exhibit a smaller free swell at 20 °C than at 60 °C. However, the results in this study demonstrate this assumption is incorrect. The actual estimated intrinsic permeability to the NaCl solution is about four times higher at 60 °C than at 20 °C. Thus, the relationships between the free swell and the hydraulic conductivity shown in previous studies (for example, Fig. 1) are not applicable at elevated temperature conditions.

The GCLs after the permeating tests are thinner for the 60 °C NaCl permeation than for the 20 °C NaCl permeation. The thicknesses of the GCL at different temperatures are actually slightly different; the thickness averaged in duplicates is 10.9 mm for the 20 °C NaCl permeation, and 10.4 mm for the 60 °C NaCl permeation.

The GCL is compressed at elevated temperature conditions. Conversely, the water contents are considerably different; the water content averaged in duplicates is 113% for the 20 °C NaCl permeation, and 99% for the 60 °C NaCl permeation. Although it can be expected that the swelling pressure will be affected by temperature, from the data presented it can be stated that temperature slightly affects the swell volume under constant load and the water retention capacity. These results and considerations are for low confining pressure levels. The temperature effects on the compressibility, including the swell volume under constant load and the water retention capacity of GCLs, for high confining pressure levels at actual landfill bottom liners may not have as large a difference as for low confining pressure levels. Future studies must examine swelling pressure and its effect on the hydraulic conductivity under elevated temperature conditions. Because the free swell is measured under non-confining pressure, the barrier performance of bentonite samples with limited deformation is related to the swelling pressure, not the free swell. In addition, the GCL after the permeating tests for the 60 °C NaCl permeation has a larger soil electric conductivity than that for the 20 °C NaCl permeation as shown in Table 4. Thus, the adsorption mass of sodium ion in the NaCl on the bentonites increases or the pore water concentration of the NaCl increases due to evaporation. Future studies must also thoroughly evaluate the water balance and the chemical composition balance of permeating solutions before and after passing through the GCLs.

5. Conclusions

This study aimed to investigate the barrier performance of GCLs against NaCl solutions at elevated temperature conditions. The effect of temperature on the hydraulic conductivity values with bentonite swelling is elucidated using the NaCl solutions, not deionized water used in previous studies, because the swelling capacity of bentonite in deionized water is so large that changes in hydraulic conductivity are negligible even at an elevated temperature.

The free swell in the 60 °C NaCl solution is larger than that in the 20 °C NaCl solution. Although previous studies have suggested that the intrinsic permeability is smaller for the 60 °C NaCl permeation than for the 20 °C NaCl permeation, the measured intrinsic permeability values of GCLs are 5.9×10^{-18} m^2 for the 20 °C NaCl permeation and 2.5×10^{-17} m^2 for the 60 °C NaCl permeation. Consequently, the intrinsic permeability increases with temperature, and the relationships between the free swell and the hydraulic conductivity reported in previous studies are not applicable to the elevated temperature condition.

Acknowledgments

We are grateful to Dr Toru Inui (Kyoto University), Dr Kazuto Endo (National Institute for Environmental Studies), and Professor Ryoichi Fukagawa (Ritsumeikan University) for their helpful comments and discussions. The supports from JSPS Grand-in-Aid for Scientific Research (Nos. 19360212 and 22360185) are gratefully acknowledged.

References

ASTM D5084, 2010. Standard Test Method for Measurement of Hydraulic Conductivity of Saturated Porous Materials Using a Flexible Wall Permeameter. American Society for Testing and Material, West Conshohocken, Pennsylvania.

ASTM D5890, 2006. Standard Test Method for Swell Index of Clay Mineral Component of Geosynthetic Clay Liners. American Society for Testing and Material, West Conshohocken, Pennsylvania.

Bear, J., 1972. Dynamics of Fluids in Porous Media. American Elsevier, New York.

Bouazza, A., Abuel-Naga, H.M., Gates, W.P., Laloui, L., 2008. Temperature effects on volume change and hydraulic properties of geosynthetic clay liners. In: Proceedings of GeoAmericas 2008 the First Pan American Geosynthetics Conference and Exhibition, Cancun, pp. 102–109.

Chien, C.C., Inyang, H.I., Everett, L.G., 2006. Barrier Systems for Environmental Contaminant Containment and Treatment. CRC Press, Boca Raton.

Cho, W.J., Lee, J.O., Chun, K.S., 1998. Influence of temperature on hydraulic conductivity in compacted bentonite. In: Proceedings of Material Research Society Symposium on the Scientific Basis for Nuclear Waste Management, Davos, vol. 506, pp. 305–311.

Cho, W.J., Lee, J.O., Chun, K.S., 1999. The temperature effects on hydraulic conductivity of compacted bentonite. Applied Clay Science 14, 47–58.

Daniel, D.E., Shan, H.-Y., Anderson, J.D., 1993. Effects of partial wetting on the performance of bentonite component of a geosynthetic clay liner. In: Geosynthetics '93 Conference Proceedings, Vancouver, vol. 3, pp. 1482–1496.

Egloffstein, T., 1995. Properties and test methods to assess bentonite used in geosynthetic clay liners. In: International Symposium on Geosynthetic Clay Liners, Nürnberg, pp. 51–72.

Egloffstein, T., 2001. Natural bentonites - influence of the ion exchange and partial desiccation on permeability and self-healing capacity of bentonites used in GCLs. Geotextiles and Geomembranes 19 (7), 427–444.

Gates, W.P., Nefiodovas, A., Peter, P., 2004. Permeability of an organo-modified bentonite to ethanol-water solutions. Clays and Clay Minerals 52 (2), 192–203.

Gleason, M.H., Daniel, D.E., Eykholt, G.R., 1997. Calcium and sodium bentonite for hydraulic containment applications. Journal of Geotechnical and Geoenvironmental Engineering 123 (5), 438–445.

Ishimori, H., Katsumi, T., Fukagawa, R., Inui, T., Endo, K., 2010. Barrier performance of GCLs against sodium chloride solutions at elevated temperature conditions. In: Proceedings of the Third International Symposium on Geosynthetic Clay Liners, Würzburg, pp. 145–154.

JBAS-107, 1991. Measuring Method of Methylene Blue Adsorption Value of Bentonite. Japan Bentonite Manufacturers Association, Tokyo.

JGS 0211, 2009. Test Method for pH of Suspended Soils. The Japanese Geotechnical Society, Tokyo.

JGS 0212, 2009. Test Method for Electric Conductivity of Suspended Soils. The Japanese Geotechnical Society, Tokyo.

JIS A1202, 2009. Test Method for Density of Soil Particles. Japanese Standards Association, Tokyo.

JIS A1203, 2009. Test Method for Water Content of Soils. Japanese Standards Association, Tokyo.

JIS A1204, 2009. Test Method for Particle Size Distribution of Soils. Japanese Standards Association, Tokyo.

JIS A1205, 2009. Test Method for Liquid Limit and Plastic Limit of Soils. Japanese Standards Association, Tokyo.

JIS A1210, 2009. Test Method for Soil Compaction Using a Rammer. Japanese Standards Association, Tokyo.

JIS A1218, 2009. Test Methods for Permeability of Saturated Soils. Japanese Standards Association, Tokyo.

Jacinto, A.C., Villar, M.V., Espina, R.G., Ledesma, A., 2009. Adaptation of the van Genuchten expression to the effects of temperature and density for compacted bentonite. Applied Clay Science 42, 575–582.

Jo, H.Y., Katsumi, T., Benson, C.H., Edil, T.B., 2001. Hydraulic conductivity and swelling of non-prehydrated GCLs permeated with single species salt solutions. Journal of Geotechnical and Geoenvironmental Engineering 127 (7), 557–567.

Katsumi, T., Fukagawa, R., 2005. Factors affecting chemical compatibility and barrier performance of GCLs. In: Proceedings of the Sixteenth International Conference on Soil Mechanics and Geotechnical Engineering, Osaka, pp. 2285–2288.

Katsumi, T., Ishimori, H., Ogawa, A., Maruyama, S., Fukagawa, R., 2008a. Effects of water content distribution on hydraulic conductivity of prehydrated GCLs against calcium chloride solutions. Soils and Foundations 48 (3), 407–417.

Katsumi, T., Ishimori, H., Ogawa, A., Yoshikawa, K., Hanamoto, K., Fukagawa, R., 2007. Hydraulic conductivity of nonprehydrated geosynthetic clay liners permeated with inorganic solutions and waste leachates. Soils and Foundations 47 (1), 79–96.

Katsumi, T., Ishimori, H., Onikata, M., Fukagawa, R., 2008b. Long-term barrier performance of modified bentonite materials against sodium and calcium permeant solutions. Geotextiles and Geomembranes 26 (1), 14–30.

Kjeldsen, P., Barlaz, M.A., Rooker, A.P., Baun, A., Ledin, A., Christensen, T.H., 2002. Present and long-term composition of MSW landfill leachate: a review. Critical Reviews in Environmental Science and Technology 32, 297–336.

Koerner, G.R., Koerner, R.M., 2006. Long term temperature monitoring of geomembranes at dry and wet landfills. Geotextiles and Geomembranes 24 (1), 72–77.

Kolstad, D.C., Benson, C.H., Edil, T.B., 2004a. Hydraulic conductivity and swell of nonprehydrated geosynthetic clay liners permeated with multispecies inorganic solutions. Journal of Geotechnical and Geoenvironmental Engineering 130 (12), 1236–1249.

Kolstad, D.C., Benson, C.H., Edil, T.B., Jo, H.Y., 2004b. Hydraulic conductivity of a dense prehydrated GCL permeated with aggressive inorganic solutions. Geosynthetics International 11 (3), 233–241.

Lee, J.M., Shackelford, C.D., 2005a. Impact of bentonite quality on hydraulic conductivity of geosynthetic clay liners. Journal of Geotechnical and Geoenvironmental Engineering 131 (1), 64–77.

Lee, J.M., Shackelford, C.D., 2005b. Concentration dependency of the prehydration effect for a geosynthetic clay liner. Soils and Foundations 45 (4), 27–41.

Mitchell, J.K., 1993. Fundamentals of Soil Behavior, second ed. Wiley Inter-Science, New York.

Müller, W.W., 2007. HDPE Geomembranes in Geotechnics. Springer-Verlag, Heidelberg.
Norrish, K., 1954. The swelling of montmorillonites. Discussions of Faraday Society 18, 120–134.
Norrish, K., Quirk, J., 1954. Crystalline swelling of montmorillonite, use of electrolytes to control swelling. Nature 173, 255–257.
Onikata, M., Kondo, M., Kamon, M., 1996. Development and characterization of multiswellable bentonite. In: Proceedings of the Second International Congress on Environmental Geotechnics, Osaka, pp. 587–590.
Petrov, R.J., Rowe, R.W., 1997. Geosynthetic clay liner (GCL) - chemical compatibility by hydraulic conductivity testing and factors impacting its performance. Canadian Geotechnical Journal 34, 863–885.
Posner, A., Quirk, J., 1964. Changes in basal spacing of montmorillonite in electrolyte solutions. Journal of Colloid and Interface Science 19, 798–812.
Rowe, R.K., 2005. Long term performance of contaminant barrier systems, 45th Rankine Lecture. Geotechnique 55 (9), 631–678.
Schwanka, M., Greenb, T.R., Matzlerc, C., Benedickterd, H., Fluhler, H., 2006. Laboratory characterization of a commercial capacitance sensor for estimating permittivity and inferring soil water content. Vadose Zone Journal 5 (3), 1048–1064.
Shan, H.-Y., Lai, Y.-J., 2002. Effect of hydrating liquid on the hydraulic properties of geosynthetic clay liners. Geotextiles and Geomembranes 20 (1), 19–38.
Slade, P.G., Quirk, J.P., 1990. The limited crystalline swelling of smectites in $CaCl_2$, $MgCl_2$ and $LaCl_3$ solutions. Journal of Colloid and Interface Science 144 (1), 18–26.
Slade, P.G., Quirk, J.P., Norrish, K., 1991. Crystalline swelling of smectite samples in concentrated NaCl solutions in relation to layer change. Clays and Clay Minerals 39 (3), 234–238.
Southen, J.M., Rowe, R.K., 2005a. Laboratory investigation of geosynthetic clay liner desiccation in a composite liner subjected to thermal gradients. Journal of Geotechnical and Geoenvironmental Engineering 131 (7), 925–935.
Southen, J.M., Rowe, R.K., 2005b. Modelling of thermally induced desiccation of geosynthetic clay liners. Geotextiles and Geomembranes 23 (5), 425–442.
Studds, P.G., Stewart, D.I., Cousens, T.W., 1996. The effect of ion valence on the swelling behavior of sodium bentonite. In: Proceedings of the Fourth International Conference on Re-use of Contaminated Land and Landfills, Edinburgh, pp. 139–142.
Vasko, S.M., Jo, H.Y., Benson, C.H., Edil, T.B., Katsumi, T., 2001. Hydraulic conductivity of partially prehydrated geosynthetic clay liners permeated with aqueous calcium chloride solutions. In: Proceedings of Geosynthetics Conference 2001, Portland, pp. 685–699.
Yasuhara, A., Shiraishi, H., N-ishikawa, M., Yamamoto, T., Uehiro, T., Nakasugi, O., Okumura, T., Kenmotsu, K., Fukui, H., Nagase, M., Ono, Y., Kawagoshi, Y., Baba, K., Noma, Y., 1997. Determination of organic components in leachates from hazardous waste disposal sites in Japan by gas chromatography mass spectrometry. Journal of Chromatography A 774, 321–332.
Yesiller, N., Hanson, J.L., Liu, W.L., 2005. Heat generation in municipal solid waste landfills. Journal of Geotechnical and Geoenvironmental Engineering 131 (11), 1330–1344.
Yeung, A.T., 1992. Diffuse double-layer equations in SI units. Journal of Geotechnical Engineering 118 (12), 2000–2005.
Yoshida, H., Hozumi, H., Tanaka, N., 1996. Theoretical study on temperature distribution in a sanitary landfill. In: Proceedings of the Second International Congress on Environmental Geotechnics, Osaka, pp. 323–328.